

# The Design of a High Heat Load Shutter for a Superconducting Wiggler Front-End

A. Gambitta, A. Turchet

*Sincrotrone Trieste, in Area Science Park, S.S. 14 Km 163.5, 34012 Trieste, Italy*

*Phone: + 39 - (0)40 - 3758676; Fax: + 39 - (0)40 - 3758565*

*E-mail: alessio.turchet@elettra.trieste.it*

## Abstract

A new superconducting wiggler will be installed in the ELETTRA storage ring; the maximum total power and power density of this new insertion device are 18.34 kW and 5.88 kW/mrad<sup>2</sup> respectively, with a 2 GeV beam energy and eventual 400 mA of beam current. This intense X-Ray synchrotron radiation requires the installation of a new shutter in the beamline front-end. The high load absorber must be fitted in a pre-existing vacuum chamber and moving frame. In this paper the design of the absorber is described and in particular the cooling system optimization used to minimize temperatures on the front face and the cooling channel surface of the shutter. A definition of the absorber design parameters and the choice of material are presented along with several designs that were evaluated using Finite Element thermal analysis. Some improvements in the piping layout are also discussed in order to reduce the pressure losses.

**Keywords:** finite element analysis, shutter, heat load

## 1. Introduction

ELETTRA is a third generation synchrotron light source whose storage ring typically operates at 2 GeV beam energy with an injected current of 350 mA. The need for a light source with higher radiation intensity and critical energy today requires the development of insertion devices with higher field strengths; superconducting technology can be used to reach these high magnetic fields. A new project at ELETTRA concerns the installation of a new beamline based on a superconducting wiggler that is currently under development in Novosibirsk (Russia). The maximum total power of this new insertion device (ID) will be 18.34 kW and the power density is 5.88 kW/mrad<sup>2</sup>. Due to these high values the installation of a new shutter in the beamline front-end is required. Several kinds of shutter design, currently operating at ELETTRA, have been evaluated and finally the modification of a pre-existing shutter frame was chosen in order to fit in the existing vacuum chamber and moving frame. Figure 1 shows the shutter assembly with the major components.

## 2. General Description

The main components (Fig. 1) of the shutter assembly are: a pneumatic actuator (1), slide shafts (2), cooling pipes (3), bellows (4), photon absorber (5), vacuum chamber (6). The pneumatic actuator is connected to the moving plate, traveling on three slide shafts, through six rods. On the moving plate it is connected to the upper flange of the bellows in which is inserted the photon absorber. The copper block of the absorber is

brazed to a hollow shaft containing the cooling tubes that is closed on the upper side by the flange connected to the bellows.

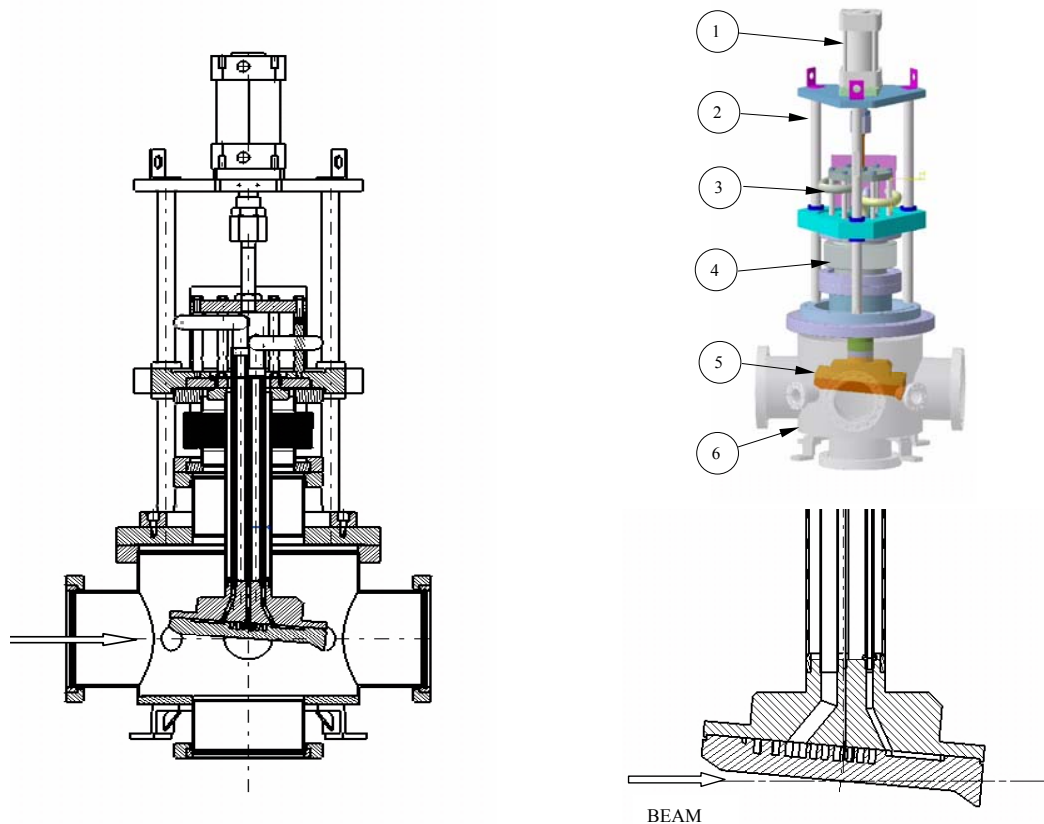


Fig. 1: Shutter assembly and photon absorber section view.

A double-acting pneumatic cylinder is used to move the photon absorber. Two limit switches are fixed on the slide shafts and two proximity switches located on the cylinder provide a position redundant signal of the shutter for the control system. The photon absorber consists of two parts brazed together: a Glidcop lower plate, with the cooling channels and an upper copper block with the pipe connections. The cooling channels are machined in the lower plate. The milled channels have a rectangular section and the pattern of the channels is designed in order to achieve a uniform cooling; for this reason the water inlets are located near the center of the plate. A safe air guard-channel is also machined around the plate and in the event of failure of the brazing this channel prevents water to enter in direct contact with the vacuum zone. A thermocouple is applied in the center of the plate as a control sensor. Since the water flow rate is very high two parallel circuits of equal working pattern are used on the Glidcop plate to limit the pressure losses. The disadvantage of this solution is that inside the hollow shaft there is four water tubes (two inlet, two outlet) two air tubes (guard-channels) plus the thermocouple and therefore the available room is minimal.

### 3. Finite Element Modeling and Thermal Analysis

Finite Element (FE) Analysis has been widely used in the evaluation of the temperature distribution during the preliminary design stage. One of the problems in using this technique is the definition of the boundary conditions. The main parameters involved are the heat flux distribution and film coefficient.

#### 3.1 Heat Load Modeling

The heat flux distribution depends on the beam power density distribution and in this design we have used the expression of Kim [1] that provides an angular distribution of power generated from undulators and wigglers. This expression is calculated for a given deflection parameter  $K$  and a numerical integration is performed to obtain a power density distribution in the plane normal to the beam axis. This function has been simplified along the vertical direction ( $y$  axis) so that the peak power density function is transformed in a step function whose value is equal to the corresponding power density peak value. The distribution used in the FEM analysis is showed in Fig. 2.

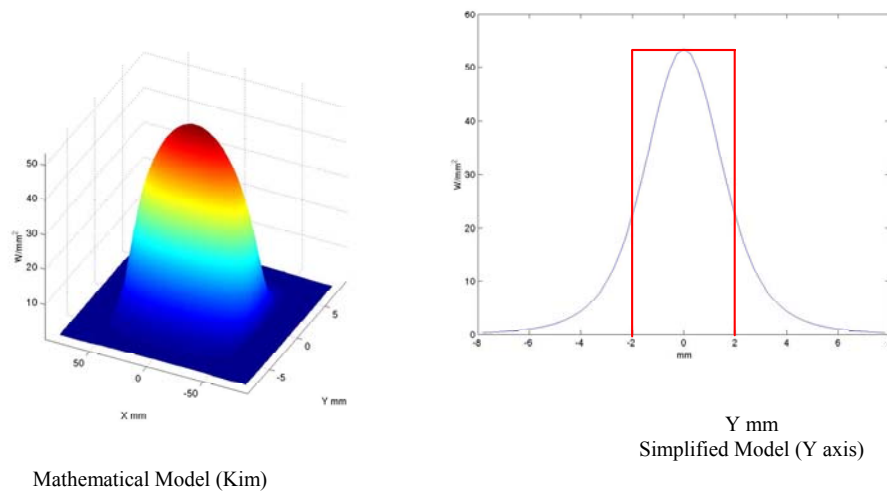


Fig. 2: Power density distribution.

#### 3.2 Film Coefficient Evaluation

The results of the thermal FE analysis is strongly affected by the value of the film coefficient inside the cooling channel, that gives a measure of the conductivity between a liquid and solid interface. Literature gives experimental relations between dimensionless groups in such cases. In particular, in forced convection, the Nusselt number (proportional to the film coefficient) is given as a function  $Nu = f(Re, Pr)$  of the Reynolds number (ratio of inertia to viscous forces,  $Re$ ) and the Prandtl number (ratio of molecular momentum to thermal diffusivity of fluid,  $Pr$ ).

In the preliminary design the Dittus and Boelter relation has been used. This relation underestimates the values for the film coefficient [2], therefore prudentially overestimate the temperature evaluation.

In the optimization process the Gnielinski equation was used, that is more precise of the previous [3], but requires an iterative process since it uses the average water film temperature (that depends on the wall temperature) and this is known only after the analysis.

## 4. Design Optimization

### 4.1 Design Parameters and Objective Functions

The design goals for the photon absorber are to obtain low surface temperatures as well as low-pressure losses in the cooling channels. In particular the objective functions in the optimization process are the maximum temperature on the channel surface ( $T_{CH}$ ) and the maximum temperature on the surface of the heated plate ( $T_{BT}$ ) [4]. The imposed constraints are:  $T_{CH} < 100^{\circ}\text{C}$  and  $T_{BT} < 300^{\circ}\text{C}$ . Another constraint is the water flow rate, which must be lower than 20 l/min in each cooling pipe. To meet these requirements we have to search for a set of design parameters values, which define the suitable design configuration.

The geometrical design variables are described in Fig. 3. Moreover the water speed  $v$  is the flow variable. The first step is to define the constant parameters in the design optimization. We have chosen to fix the pitch angle ( $\alpha = 5^{\circ}$ ) and the water speed ( $v = 6$  m/sec).

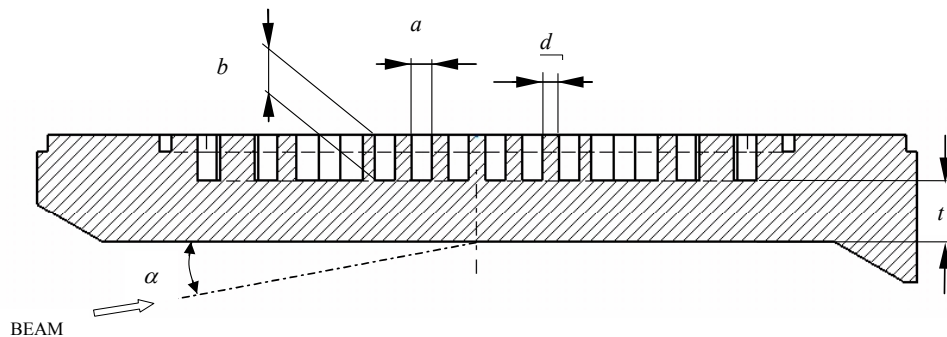


Fig. 3: Design parameters.

### 4.2 Influence of Design Parameters

A sensitivity analysis has been performed before starting with the optimization process to identify the most important parameters. The sensitivity analysis has been

carried out with several FE simulations using a parameterized model. The checked parameters were  $D_{eq}$  (equivalent diameter for the rectangular channel cross section),  $\Lambda = a/b$  (channel aspect ratio),  $t$  (thickness of shutter plate),  $d$  (distance between channels in the cross section). These tests have shown that the chosen set of design variables (channel width  $a$ , thickness  $t$ ) were efficiently fulfilling the requested design goals, while the parameter  $d$  revealed a low influence on the objective function. The aspect ratio parameter  $\Lambda$  was further investigated. As a matter of fact the best performance was achieved with low values of  $\Lambda$ , but upon consideration of the drop in pressure inside the channel (that increases with decreasing  $\Lambda$ ) suggested us to fix this parameter at  $\Lambda = 0.5$ .

### 4.3 Optimization Process

The design process begins with the calculation of a proposed starting design. The film coefficient is calculated with the Gnielinski equation, assuming an average film temperature  $T_F = 20\text{ }^\circ\text{C}$ . This first FE model gives the temperature distribution field in the shutter; from the calculated wall temperatures in the channels the  $T_F$  value is recalculated for a second, more precise FE result.

The maximum temperature on the channel surface ( $T_{CH}$ ) and the maximum temperature on the shutter ( $T_{BT}$ ) are compared with the imposed constraints. The design variables are then modified in order to meet these conditions. If  $T_{BT} > 300\text{ }^\circ\text{C}$  the thickness  $t$  is reduced, while if  $T_{CH} > 100\text{ }^\circ\text{C}$  the channel width  $a$  is reduced. Finally the pressure drop  $\Delta p$  is calculated. If the pressure drop is too high (compared with the available pressure in the manifold, about 8 bar for ELETTRA), the width  $a$  and the distance  $d$  are increased. The optimum design will be achieved when all the conditions are satisfied ( $T_{BT} < 300\text{ }^\circ\text{C}$ ,  $T_{CH} < 100\text{ }^\circ\text{C}$ ,  $\Delta p < 8\text{ bar}$ ).

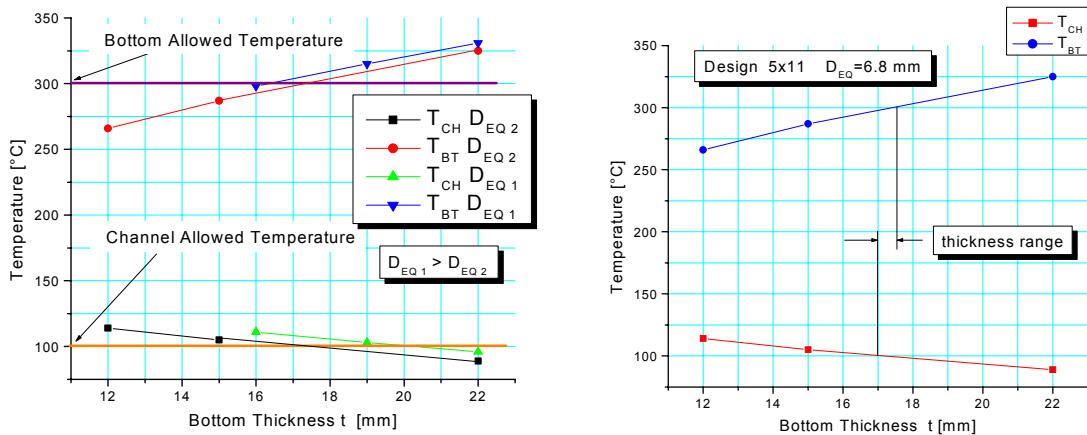


Fig. 4: Temperature  $T_{CH}$   $T_{BT}$  versus bottom thickness  $t$ .

Experience showed that the best way to start the design process is to use relatively large values for the channel width  $a$  (therefore a large value of  $D_{eq}$ ) and small values for the thickness  $t$ . The curves obtained from the simulation, see Fig. 4, represent  $T_{BT}$  and

$T_{CH}$  values versus  $t$ . By decreasing the  $D_{eq}$  parameter these two curves move down and finally intersect the temperature constraint limits. It is then possible to define an available range of values for the thickness  $t$ . This range increases with a lower value of  $D_{eq}$  but decreasing this parameter also means an increase of  $\Delta p$ . Moreover, since the water speed is fixed, the flow rate is reduced and therefore the temperature rise of the water can reach undesirable values.

Another interesting plot of  $T_{CH}$  versus  $T_{BT}$  is presented in Fig. 5. This figure shows a set of points representing the evaluated designs. It can be noted that all points with the same  $D_{eq}$  are aligned. By decreasing  $D_{eq}$  the corresponding curve moves down and intersects the rectangular zone of possible designs for values of  $D_{eq} < 6.8$  mm. With this approach the optimum design is obtained by searching for the maximum  $D_{eq}$  that provides a design located inside this zone. This optimum design satisfies the imposed constraints and the minimum  $\Delta p$ . In our approach we have preferred to penalize the maximum temperature values with respect to the pressure drop, because  $\Delta p$  has some degree of uncertainty and will be increased by the pressure drop of the external connection circuits. Therefore a wide safety margin is considered.

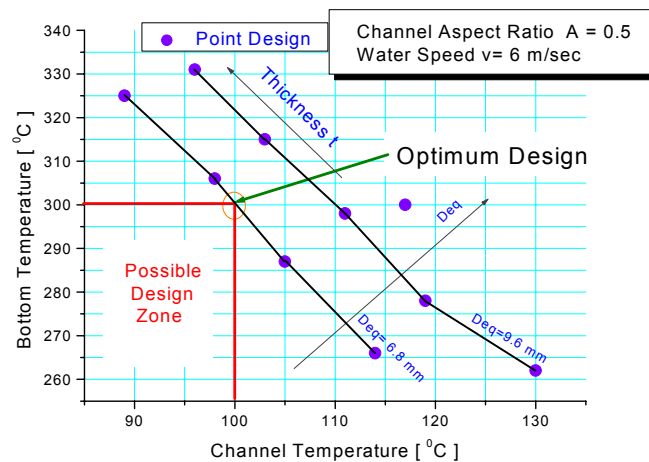


Fig. 5:  $T_{BT}$  versus  $T_{CH}$  for different designs and  $D_{eq}$ .

The results for the final design are summarized in Table 1. The design parameters were fixed at the following values:  $a = 5$  mm;  $b = 11$  mm;  $t = 15$  mm;  $d = 4$  mm.

Table 1: Results for the Final Design

Water speed [m/s]	Flow rate [l/min]	Water $\Delta T$ [°C]	Press. $\Delta p$ [bar]	$T_{BT}$ [°C]	$T_{CH}$ [°C]
6	39.6	7.2	3	287	98

Finally, Fig. 6 shows the FEM results of the final design.

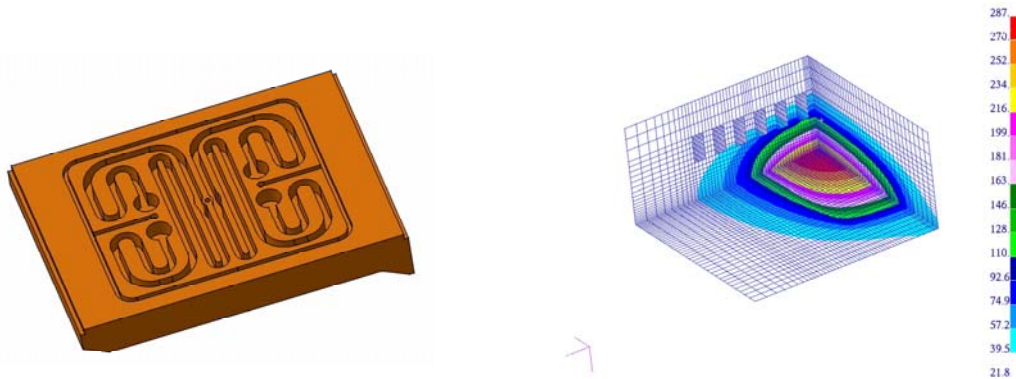


Fig. 6: Final design and FEM thermal analysis.

## 5. Conclusions

FE analysis is usually carried out only to verify the final design that is the product of the experience of the analyst. An alternative approach is presented here, based on a process of optimization that can be of general interest for similar developments permitting a guide to the final design. Of course many optimization processes are possible starting from different sets of variables, however, we hope to stimulate the search for a common strategy to be found for similar developments.

## 6. Acknowledgements

The authors would like to thank Massimiliano Tudor and Omar Zuppan for their effort and technical support in this work.

## 7. References

- [1] K. J. Kim, "Angular Distribution of Undulator Power for an Arbitrary Deflection Parameter K," Nucl. Instrum. Methods in Physics Research A246 (1986) 67-70.
- [2] W. M. Rohsenow, J. P. Hartnett, E. N. Ganic, Handbook of Heat Transfer Fundamentals, 2nd Ed., McGraw-Hill, New York, 1985.
- [3] W. M. Rohsenow, J. P. Hartnett, Handbook of Heat Transfer Application, 2nd Ed., McGraw-Hill, New York, 1985.
- [4] S. Sharma, E. Rotela, and A. Barcikowski, "High Heat-Load Absorbers for the APS Storage Ring," Proceedings of the 1st International Workshop on Mechanical Engineering Design of Synchrotron Radiation Equipment and Instrumentation, July 2000, pp 5-10.